Transactions **of the SMiRT 27**
Yokohama, Japan, March 3-8, 2024
Division II

CONTACT AND FRACTURE MECHANICAL ANALYSES OF A CLADDING FAILURE IN PCMI

Hyung-Kyu Kim[1]

[1] Principal Researcher, Korea Atomic Energy Research Institute, Daejeon, Korea (hkkim1@kaeri.re.kr)

ABSTRACT

Analysis method of a cladding crack subject to PCMI is studied. A surface perpendicular edge crack emanated from the sharp edge of a cracked pellet fragment is considered, which is in contact with the cladding inner surface. Essential tasks are i) the stress singularity at the sharp contact edge, ii) traction free condition on the free surfaces, and iii) numerical technique for singular integral equations. They are resolved, in order, by constituting an eigenvalue problem, deriving corrective influence functions using pseudo dislocations and applying a numerical technique widely used in crack analysis. Finally, equation form of the stress intensity factors of a cladding crack are derived. An example calculation is provided.

INTRODUCTION

The term, "pellet-cladding mechanical interaction (PCMI)" is used when a contact between the pellets and cladding tubes of a fuel rod takes place. It is attributed to the difference in deformation of the pellets and cladding tubes. So to speak, the PCMI occurs when the outward expansion of the cylindrical pellets is greater than that of the cladding tubes during reactor operation. The expansions are caused by a thermal effect for both pellets and cladding tubes, and an irradiation (swelling) is another significant effect of the pellet expansion. The contact can cause a crack initiation in the cladding tubes due to a high stress. If the crack penetrates the cladding tubes, radioactive fission gases are released out to the reactor coolant. Therefore, a cladding cracking failure due to PCMI needs to be strictly controlled.

When the contact between the pellets and cladding tubes are investigated in further detail, it is generally found that the pellets have cracks because of its ceramic character and a sharp edge of the cracked pellet presses the inner surface of the cladding tubes. This significantly increases the cladding stress locally at the sharp edge, which results in a higher propensity to cracking failure of the cladding tubes as illustrated in figure 1. The localized high stress at the pellet sharp edge has been widely concerned in the previous PCMI studies by Gittus (1972), Roberts (1978), Nakatsuka (1981), Ranjan and Smith (1980), Walker et al. (1992), Marchal et al. (2009) and Sercombe et al. (2012). They commonly dealt with a stress concentration with a certain number of concentration factor for the localized stress at the location of the sharp edge.

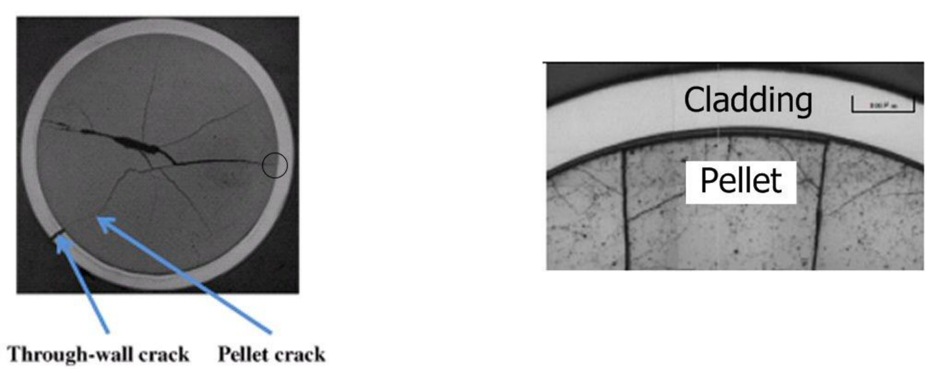

Figure 1. Typical view of the PCMI.

However, stringently speaking, a singular stress is to occur if the edge radius is null (in theory), i.e. the case of a sharp edge. It is analogous to the singular stress at a crack tip. Therefore, a stress intensification is necessarily considered in the PCMI contact problem. A contact problem dealing with a sharp edge has been studied such as Churchman and Hills (2006), Karuppanan et al. (2008) and Flicek et al. (2015) for the case of elastically similar materials' contact, and Kim et al. (2014) and Kim and Kim (2014) for the case of elastically dissimilar materials' contact. They commonly used an asymptotic analysis method where an eigenvalue problem was constituted using a stress potential developed by Williams (1952). This work also adopted the method for the contact analysis.

In turn, a crack problem needs to be tackled, which initiates at the location of the sharp edge and grew into the cladding tubes. In this work, the cladding crack was simulated as a continuous distribution of pseudo edge dislocations, and a dislocation density function technique was used. One of the difficulties was to perform traction free conditions at the free boundaries formed at the crack surface of the pellet and cladding inner surface. To resolve the difficulty, a technique of applying pseudo-dislocations to the free surfaces was applied once again, which has been tried by Churchman et al. (2006), for the case of a contact of elastically similar materials. A key of this technique was to derive a correction function to make the resultant stresses on the free surfaces disappear. However, it cannot be directly applied to the present case of elastically dissimilar materials' contact of the PCMI. Instead, a finite element analysis was used here.

The purpose of this work is to show a novel method to calculate the stress intensity factors of a crack in the cladding tubes which is subject to an indentation by cracked pellets, simulating the PCMI condition. In particular, the sharp edge of a cracked pellet fragment and the traction free conditions at the pellets and cladding tubes are brought into focus, which can provide a mechanically stringent analysis. Thus, contact mechanics and fracture mechanics are sequentially consulted. As a result, formulae of the stress intensity factors of the cladding crack is derived using the stress intensity factors due to the sharp edge contact, together with the eigen-solutions obtained for the PCMI contact configuration.

ANALYSIS SCHEME

The geometrical model of the present problem is illustrated in figure 2. The cladding tube including a crack and fragment of a cracked pellet having a sharp edge are modelled as a half plane including a crack and a wedge having an edge angle, φ, respectively. The cladding tube and pellet are denoted as body 1 and 2, respectively, and whose elastic properties are described as E_i and ν_i, (i = 1,2; the subscript i identifies the body number) where E and ν are the elastic modulus and Poisson ratio, respectively. Polar coordinates are chosen such that the origin is at the contact location of a sharp edge, where the cladding crack initiates, as is often observed in the PCMI cladding failure (see figure 1). The angle, θ, increases from a surface normal of the half plane in a counter-clockwise sense. The cladding crack has an angle, ψ, from the surface normal of the half plane. It is assumed that the contact between the pellets and cladding tubes is adhered because it can be readily assumed that there is no slipping on the contact surface when the PCMI takes place.

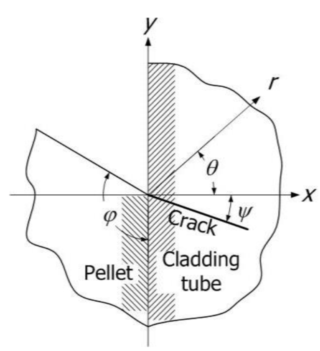

Figure 2. Geometrical description of the contact between cracked pellet fragment and cladding tube.

A normal contact force exists on the contact surface of body 1 and 2 owing to the larger expansion of the pellets than the cladding tubes. Simultaneously, a tensile stress exists in the cladding tube along the y direction owing to thermal expansion. On the other hand, the cladding crack can be simulated as a continuous distribution of pseudo-edge dislocations. The stress potential due to an edge dislocation, developed by Dundurs (1969), can be used to evaluate the stresses induced by the pseudo-dislocations on the crack line. Now, to analyse the cladding crack of length, c, a traction free condition on the crack line is used with a superposition principle developed by Bueckner (1958). Consequently, governing equations of the present problem are written as follows, and figure 3 shows the decomposition of the present problem reflecting the Bueckner principle.

$$\sigma_{\theta\theta}^{D} + \sigma_{\theta\theta}^{C} + \sigma_{\theta\theta}^{T} = 0, (0 \leq r \leq c, \theta = -\psi), \tag{1a}$$
$$\sigma_{r\theta}^{D} + \sigma_{r\theta}^{C} + \sigma_{r\theta}^{T} = 0, (0 \leq r \leq c, \theta = -\psi) \tag{1b}$$

where the superscript, D, C and T mean the dislocation, contact and thermal-induced, in order. The stress components, $\sigma_{\theta\theta}$ and $\sigma_{r\theta}$ take the roles of opening and slipping of the crack faces, respectively, and thus the mode I and II stress intensity factors (i.e., K_I and K_{II}) are to be evaluated from equations (1a) and (1b), respectively.

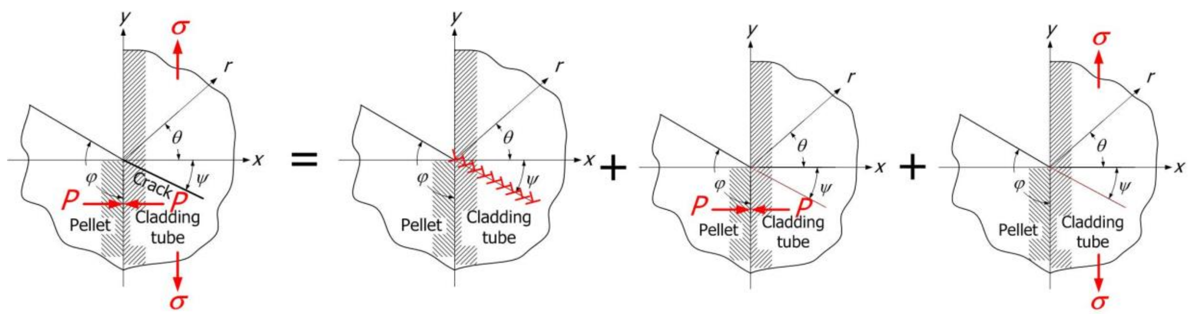

Figure 3. Illustration of the Bueckner principle presently used: (a) for σ_{ij}^{D} (b) for σ_{ij}^{C} (c) for σ_{ij}^{T}.

The mode I and II stress intensity factors of the cladding crack are obtained using the followings.

$$K_{I}^{\text{crack}} = \lim_{r \to 0} \left[\sigma_{\theta\theta}(r, \theta = -\psi) \cdot \sqrt{r} \right] \tag{2a}$$
$$K_{II}^{\text{crack}} = \lim_{r \to 0} \left[\sigma_{r\theta}(r, \theta = -\psi) \cdot \sqrt{r} \right]. \tag{2b}$$

Presently, the edge angle of the pellet fragment is set as $\varphi = \pi/2$, and that of the cladding crack is $\psi = 0$ which are often observed in the irradiated fuel rod. However, it may be noted that the present analysis method and process will not be altered even if φ and ψ change.

CONTACT MECHANICAL ANALYSIS

First, $\sigma_{\theta\theta}^{C}$ and $\sigma_{r\theta}^{C}$ are to be calculated. This process can be done by formulating an eigenvalue problem. An Airy stress potential originally developed by Williams (1952) for a sharp notch in a homogeneous body is modified to apply for a contact of a sharp wedge and an elastically dissimilar half plane, as given below.

$$\Phi_n = r^{\lambda+1}\{a_n \cos(\lambda+1)\theta + b_n \sin(\lambda+1)\theta + c_n \cos(\lambda-1)\theta + d_n \sin(\lambda-1)\theta\}, \ (n = 1,2) \tag{3}$$

where Φ is the Airy stress potential, λ and $a_n \sim d_n$ are the constants to be determined. The subscript, n denotes the body number (1: cladding tube, 2: pellet). The stress and displacement equations are derived as follows, using the relationship between the Airy stress potential and stresses ($\sigma_{ij};\ \ i,j = r,\theta$) and displacements ($u_i;\ \ i = r,\theta$).

$$\sigma_{rr}^n = r^{\lambda-1}[a_n\{-\lambda(\lambda+1)\}\cos(\lambda+1)\theta + b_n\{-\lambda(\lambda+1)\}\sin(\lambda+1)\theta + c_n\{-\lambda(\lambda-3)\}\cos(\lambda-1)\theta + d_n\{-\lambda(\lambda-1)\}\sin(\lambda+1)\theta], \tag{4a}$$

$$\sigma_{\theta\theta}^n = r^{\lambda-1}[a_n\{\lambda(\lambda+1)\}\cos(\lambda+1)\theta + b_n\{\lambda(\lambda+1)\}\sin(\lambda+1)\theta + c_n\{\lambda(\lambda+1)\}\cos(\lambda-1)\theta + d_n\{\lambda(\lambda+1)\}\sin(\lambda-1)\theta], \tag{4b}$$

$$\sigma_{r\theta}^n = r^{\lambda-1}[a_n\{\lambda(\lambda+1)\}\sin(\lambda+1)\theta + b_n\{-\lambda(\lambda+1)\}\cos(\lambda+1)\theta + c_n\{\lambda(\lambda-1)\}\sin(\lambda-1)\theta + d_n\{-\lambda(\lambda-1)\}\cos(\lambda-1)\theta] \tag{4c}$$

$$u_r^n = \frac{r^\lambda}{2G_n}[-a_n(\lambda+1)\cos(\lambda+1)\theta - b_n(\lambda+1)\sin(\lambda+1)\theta + c_n(\kappa_n-\lambda)\cos(\lambda-1)\theta + d_n(\kappa_n-\lambda)\sin(\lambda-1)\theta] \tag{4d}$$

$$u_\theta^n = \frac{r^\lambda}{2G_n}[a_n(\lambda+1)\sin(\lambda+1)\theta - b_n(\lambda+1)\cos(\lambda+1)\theta + c_n(\kappa_n+\lambda)\sin(\lambda-1)\theta + d_n(\kappa_n+\lambda)\cos(\lambda-1)\theta] \tag{4e}$$

where the super- or subscript, n denote the body number. With discarding it for simplicity, G is the shear modulus, and κ is the Kolosov constant defined as $(3-4\nu)$ for plane strain and $(3-\nu)/(1+\nu)$ for plane stress conditions with ν being the Poisson ratio.

Using $\varphi = \pi/2$, the boundary conditions of the present contact problem are written as follows.

$$\begin{gathered} \sigma_{\theta\theta}^1(r,\pi/2) = 0,\ \sigma_{r\theta}^1(r,\pi/2) = 0,\ \sigma_{\theta\theta}^2(r,-\pi) = 0,\ \sigma_{r\theta}^2(r,-\pi) = 0 \\ \sigma_{\theta\theta}^1(r,-\pi/2) - \sigma_{\theta\theta}^2(r,-\pi/2) = 0,\ \sigma_{r\theta}^1(r,-\pi/2) - \sigma_{r\theta}^2(r,-\pi/2) = 0, \\ u_r^1(r,-\pi/2) - u_r^2(r,-\pi/2) = 0,\ u_\theta^1(r,-\pi/2) - u_\theta^2(r,-\pi/2) = 0. \end{gathered} \tag{5a-h}$$

Equations (5a-h) constitute a simultaneous equation that consists of eight homogeneous equations with eight unknown constants, $a_1 \sim d_2$ and λ. Algebraically, the determinant of the coefficient matrix of the simultaneous equation should be null to have non-trivial solutions, which results in a polynomial equation of λ only. The solutions of λ that are smaller than 1 give singular stresses due to the term, $r^{\lambda-1}$ (equations (4a-c)). Thus, the value, $(1-\lambda)$ determines the order of stress singularity. On the other hand, if the contact is adhered like the present PCMI case, there appears two λ's, which are smaller than 1.

As for the material properties of the present PCMI problem, E_1 = 76333.3 MPa, ν_1 = 0.3; E_2 = 177710 MPa, ν_2 = 0.3 were used for the zircaloy-4 cladding tubes and UO_2 pellets. As a result, λ_I = 0.508 and λ_{II} = 0.807 (for $\lambda < 1$) were obtained. When those were substituted back into the original equations (5a-h), the unknown constants, $a_1 \sim d_2$ were evaluated. It is noted here that the constants reveal the eigen-solutions and thus, they can be evaluated as the proportional values with respect to one of them. In the present analysis, the constants were normalized by a_1. Then, the form of stress equations were written as

$$\sigma_{\theta\theta}^C = K_I^{\text{contact}} r^{-0.492} f_{\theta\theta}^I(\theta) + K_{II}^{\text{contact}} r^{-0.193} f_{\theta\theta}^{II}(\theta) \ \text{+ non-singular terms} \tag{6a}$$

$$\sigma_{r\theta}^C = K_I^{\text{contact}} r^{-0.492} f_{r\theta}^I(\theta) + K_{II}^{\text{contact}} r^{-0.193} f_{r\theta}^{II}(\theta) \ \text{+ non-singular terms} \tag{6b}$$

In equations (6a) and (6b), K_I^{contact} and K_{II}^{contact} are the scaling factors to the eigen-stresses to incorporate the actual contact loads, and are called generalized stress intensity factors of mode I and II, respectively. $f_{ij}^M(\theta)$, (M = I, II; $i,j = r,\theta$) is an angular function which reveals spatial variation of the stresses in the problem domain, presently, $-\pi \le \theta \le \pi/2$, which is illustrated in figure 4. The terms in equations (6a) and (6b) that do not include K_I^{contact} and K_{II}^{contact} are the non-singular bounded terms which appear for λ's that are greater than 1. Those become considerably smaller than the singular terms as $r \to 0$.

Therefore, we can discard the non-singular terms as we are focusing on the very small localized region around the sharp edge to consider the cladding failure due to the contact of a sharp edge of the cracked pellet.

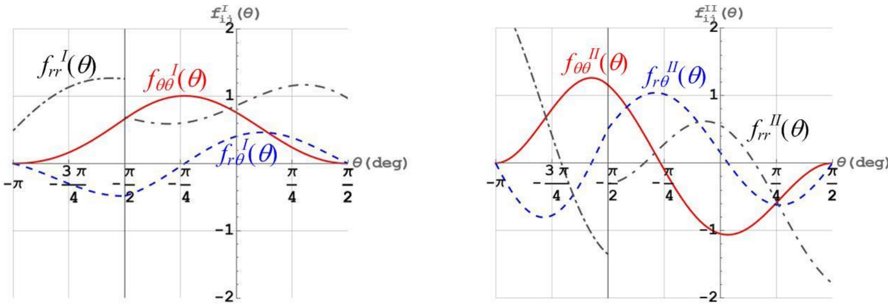

Figure 4.The angular functions, $f_{ij}^{I}(\theta)$ and $f_{ij}^{II}(\theta)$, (i,j = r,θ) of the present problem.

In turn, K_I^{contact} and K_{II}^{contact} are to be evaluated after finding the specific angles, θ_I and θ_{II} such that $f_{\theta\theta}^{II}(\theta_I) = f_{r\theta}^{I}(\theta_{II}) = 0$. This gives θ_I = -42.1° and θ_{II} = -48.3°, which can be read from figure 4. Then, the final K_I^{contact} and K_{II}^{contact} are obtained from the following equations.

$$K_I^{\text{contact}} a^{\lambda_I - 1} = K_I^{\text{contact}} a^{-0.492} = \Lambda_I \sigma_o = \lim_{r\to 0}\left[\sigma_{\theta\theta}(r,\theta_I)\cdot r^{1-\lambda_I}\right]\cdot\sigma_o \tag{7a}$$

$$K_{II}^{\text{contact}} a^{\lambda_{II} - 1} = K_{II}^{\text{contact}} a^{-0.193} = \Lambda_{II} \sigma_o = \lim_{r\to 0}\left[\sigma_{r\theta}(r,\theta_{II})\cdot r^{1-\lambda_{II}}\right]\cdot\sigma_o \tag{7b}$$

where Λ_I and Λ_{II} are found from $\lim_{r\to 0}\left[\sigma_{\theta\theta}(r,\theta_I)\cdot r^{1-\lambda_I}\right]$ and $\lim_{r\to 0}\left[\sigma_{r\theta}(r,\theta_{II})\cdot r^{1-\lambda_{II}}\right]$ in figure 4, respectively. They can be obtained from finite element analysis (FEA) with using a simple and finite geometry that has the same contact conditions (i.e., material properties, adhesion, and φ). σ_o and a are the uniform contact stress and contact length, respectively.

Figure 5 depicts the finite element model and figure 6 shows the result from which $\Lambda_I = -1.2570$ and $\Lambda_{II} = 0.4076$ are found.

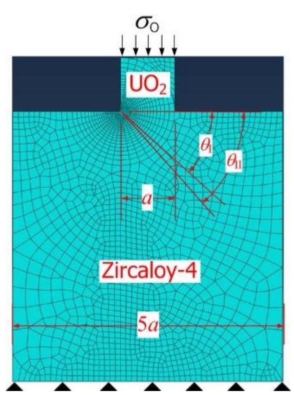

Figure 5. Finite element model
(a = 20 mm, θ_I = -42.1°, θ_{II} = -48.3°, σ_o = 1 MPa).

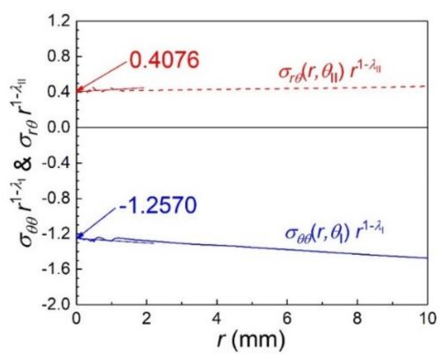

Figure 6. Λ_I and Λ_{II}.

As a result, the stress components due to the present PCMI contact are expressed as follows. It is noted that only the singular terms are written here.

$$\sigma_{\theta\theta}^{C} = \left[-1.257(r/a)^{-0.492} f_{\theta\theta}^{I}(\theta) + 0.408(r/a)^{-0.193} f_{\theta\theta}^{II}(\theta)\right]\cdot\sigma_o \tag{8a}$$

$$\sigma_{r\theta}^{C} = \left[-1.257(r/a)^{-0.492} f_{r\theta}^{I}(\theta) + 0.408(r/a)^{-0.193} f_{r\theta}^{II}(\theta)\right] \cdot \sigma_o \quad (8b)$$

where, in the actual PCMI case, σ_o means the contact stress exerted to the inner surface of the cladding tube owing to the swelling and thermal expansion of the pellet, and a means the arc length of the contact region between the cracked pellet fragment and cladding inner surface.

In the FEA, σ_o = 1 MPa was simply applied to obtain the Λ_I and Λ_{II}. However, it is hard to know the actual contact stress which is caused by the expansion of the pellet in the case of the PCMI. Here, 10 MPa was tentatively applied for σ_o, which was used by Roberts (1978) in his calculation of the cladding stresses subject to PCMI. Also, a = 3.283 mm was used with assuming the pellet was cracked into 8 equally spaced fragments along the outer surface whose diameter was 8.36 mm, often used for a cladding tube of 9.5 mm in its outside diameter. Such equally spaced fragments of a pellet has been often used in the previous researches by Marchal et al. (2009) and Sercombe et al. (2012).

FRACTURE MECHANICAL ANALYSIS

Equations (8a) and (8b) will provide the normal and shear stresses on the cladding crack due to the contact of the pellet having a sharp edge when $0 \leq r \leq c, \theta = -\pi/2$ are applied. In turn, the normal and shear stresses due to the pseudo-dislocations distributed along the cladding crack are evaluated in this section. To this end, another Airy stress function due to an edge dislocation in an infinite domain can be primarily used, which has been developed by Dundurs and Sendeckyj (1965) for a bimetallic problem. The stress components are neatly found in Hills et al. (1996) under the Cartesian coordinates system illustrated in figure 7 below where, in the left, a single edge dislocation on the positive x axis denotes one of the distributed dislocations, shown in the right, to simulate the cladding crack.

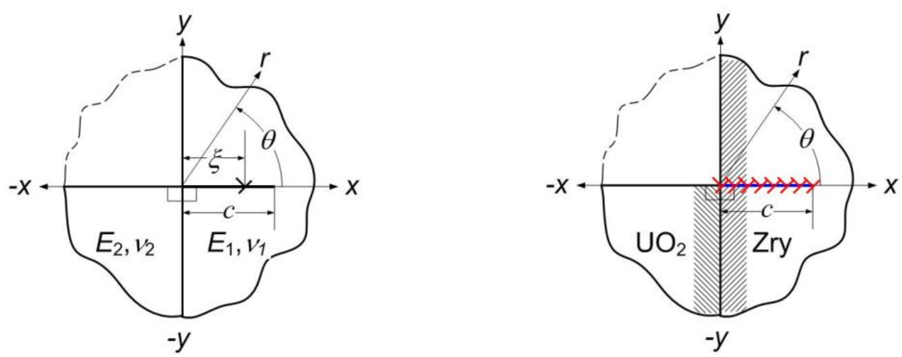

Figure 7.Geometrical model and coordinates used for the cladding crack analysis (left): the subscript “1” and “2” of E and ν denote the zircaloy-4 cladding tubes and UO_2 pellets. Also, the model for the present analysis is given (right) where a cladding crack of length c is described as a distributed edge dislocations.

The resultant stress components in the cladding tube due to an edge dislocation at $x = \xi$, $y = 0$ are given below. Here, the superscript, (1) denotes the body 1, i.e. the zircaloy-4 cladding tube.

$$\sigma_{ij}^{(1)}(x,y;\xi,0) = \frac{2G_1}{\pi(\kappa_1+1)}\left\{G_{xij}^{(1)}(x,y;\xi,0)b_x(\xi,0) + G_{yij}^{(1)}(x,y;\xi,0)b_y(\xi,0)\right\}, (i,j) = (x,y) \quad (9)$$

where G_1, and κ_1 re the shear modulus and Kolosov’s constant of the zircaloy-4 cladding tube, respectively. b_x and b_y are the x- and y components of the Burgers vector of the edge dislocation, respectively. The lengthy expressions of the $G_{kij}^{(1)}(x,y;\xi,0), (k = x,y), (i,j) = (x,y)$ can be found in Equation. (A.8) of the Appendix A.3 in Hills et al. (1996).

Key issue is to compose a traction free conditions on the free boundaries ($-\infty < x \leq 0,\ 0 < y \leq \infty$ in figure 7) due to the cracked pellet fragment. This can be resolved by applying again a continuous distribution of edge dislocations along the free boundaries. The stresses by the dislocations on the boundaries are to be added to the stresses due to a dislocation on the cladding crack $(x = \xi, y = 0)$, and set the sum to null on the free boundaries, which resultantly gives correction terms due to the free boundaries. Then, the final equations are written as

$$\sigma_{ij}^{(1)}(x,0;\xi,0) = \frac{2G_1}{\pi(\kappa_1+1)}\Big[\Big\{G_{xij}^{(1)}(x,0;\xi,0) + F_{xij}(x,\xi)\Big\}b_x(\xi,0) + \Big\{G_{yij}^{(1)}(x,0;\xi,0) + F_{yij}(x,\xi)\Big\}b_y(\xi,0)\Big], (i,j) = (x,y), \quad (10)$$

where $F_{xij}(x,\xi)$, $F_{yij}(x,\xi)$ are the correction terms (functions) for the *x*- and y components of the Burgers vectors of the dislocations along the free boundaries.

However, it is extremely hard to analytically evaluate the correction terms owing to the dislocations along the bimetallic interface (esp. $0 < y \leq \infty$). The Dirac delta function and Cauchy singular integral equation of the second kind appear, and a numerical solution technique has not been well developed. Instead, an FEA was used to numerically obtain $F_{xij}(x,\xi)$ and $F_{yij}(x,\xi)$ using a simple model as illustrated in figure 8. Pseudo-dislocations artificially applied to the free boundaries for a traction-free are also graphically explained (figure 8, right). The idea of the FEA method is described in equation (11).

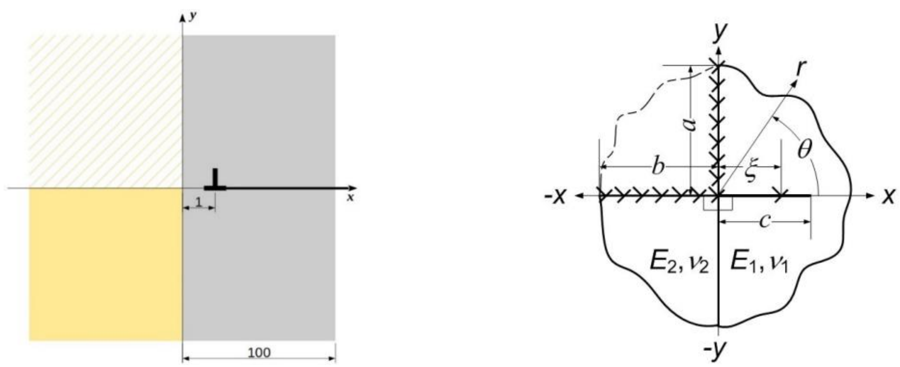

Figure 8. Finite element model to evaluate the correction terms of the present crack problem (left) and illustration of the applied dislocations on the free boundaries (right).

$$F_{kij}(x,\xi) = \frac{2G_1}{\pi(\kappa_1+1)}\Big\{\sigma_{ij}(x,0;\xi,0)\big|_{\text{infinite}} - \sigma_{ij}(x,0;\xi,0)\big|_{\text{truncated}}\Big\}, (i,j) = (x,y) \quad (11)$$

for each Burgers vector component, b_k ($k = x,y$). In equation (11), the subscript, "infinite" means the full domain of the 200×200 square whereas the "truncated" does the domain where, in figure 8, the 2nd quadrant (hatched region) is subtracted from the full domain of the FE model. The 3rd quadrant in yellow is the cracked pellet fragment, and the 1st and 4th quadrants in grey display the cladding tube in the FE model.

Resultantly, $F_{xij}(x,\xi)$ and $F_{yij}(x,\xi)$ are obtained in a numeric form. It is necessary to express them as a function form to use in equation (10). A following polynomial form was considered for it.

$$F_{kij}(\hat{x}) = \frac{1}{\hat{x}^{1-\lambda_I}+\hat{x}^1}\sum_{m=0}^{3} C_m\left(\frac{\hat{x}}{1+\hat{x}}\right)^m, \ (m = 3;\ \hat{x} = x/\xi\ ;\ k = x,y; i,j = x,y). \quad (12)$$

Figure 9 shows $F_{xyy}(\hat{x})$, $F_{xxy}(\hat{x})$, $F_{yyy}(\hat{x})$, $F_{yxy}(\hat{x})$ where $\hat{x} = x/\xi$, and the coefficients in equation (12) after curve-fitting.

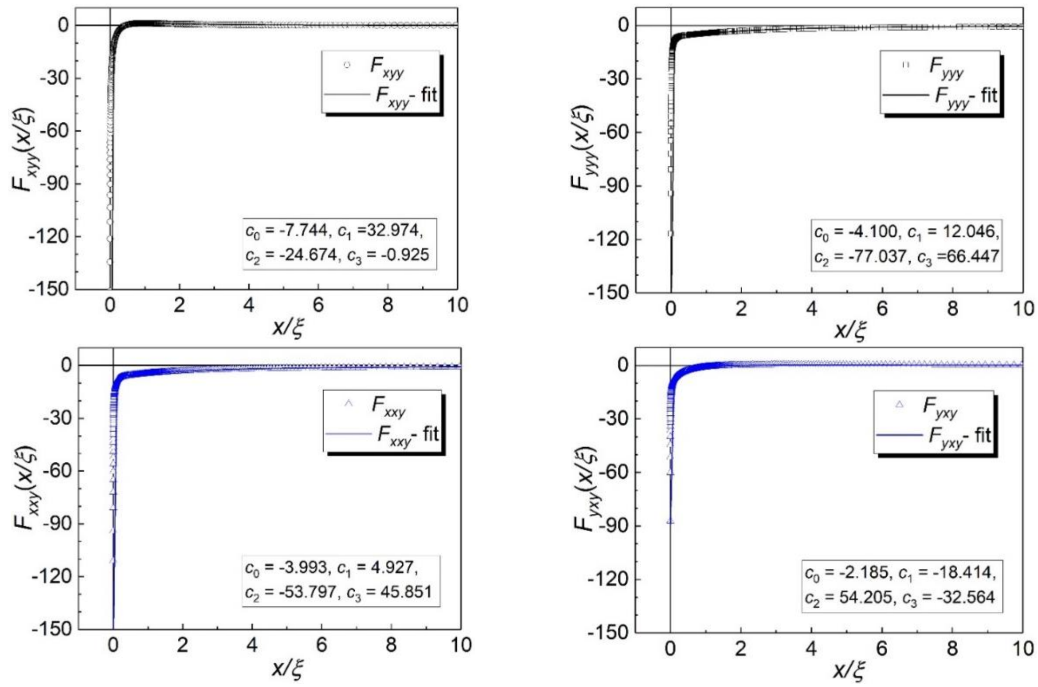

Figure 9. Plots of $F_{kij}(\hat{x}),(\hat{x} = x/\xi\,;\ k = x, y; i, j = x, y)$ and the coefficients of equation (12).

Now the resultant equations for opening and shearing modes of the cladding crack are written as follows, reflecting equations (1a) and (1b).

For opening mode, from $\sigma_{yy}(x,0) = 0$ $(0 \le x \le c)$:

$$K_I^0 x^{\lambda_I - 1} + K_{II}^0 x^{\lambda_{II}-1} + \sigma_{yy}^T(x,0)$$
$$+\frac{2G_1}{\pi(\kappa_1+1)}\int_0^c \left[\left\{G_{xyy}^{(1)}(x,0;\xi,0) + F_{xyy}(x,\xi)\right\}B_x(\xi) + \left\{G_{yyy}^{(1)}(x,0;\xi,0) + F_{yyy}(x,\xi)\right\}B_y(\xi)\right]d\xi = 0,$$
$$(0 \le x \le c) \qquad (13a)$$

and for shearing mode, from $\sigma_{xy}(x,0) = 0$ $(0 \le x \le c)$:

$$K_I^0 x^{\lambda_I - 1} g_{r\theta}^I + K_{II}^0 x^{\lambda_{II}-1} g_{r\theta}^{II}$$
$$+\frac{2G_1}{\pi(\kappa_1+1)}\int_0^c \left[\left\{G_{xxy}^{(1)}(x,0;\xi,0) + F_{xxy}(x,\xi)\right\}B_x(\xi) + \left\{G_{yxy}^{(1)}(x,0;\xi,0) + F_{yxy}(x,\xi)\right\}B_y(\xi)\right]d\xi = 0,$$
$$(0 \le x \le c) \qquad (13b)$$

where $B_x(\xi)$ and $B_y(\xi)$ are the dislocation density functions due to Burgers vector components, b_x and b_y, respectively, of an edge dislocation at $x = \xi$ in the crack line. $\sigma_{yy}^T(x,0)$ is the thermal hoop (tensile) stress in the cladding tube. It is noted that the thermal expansion does not affect shear stress so it does not appear in equation (13b). K_I^0 and K_{II}^0 are the generalized stress intensity factors due to the sharp edge contact rescaled along the crack line ($\theta = 0$). They are evaluated from $K_I^0 = K_I^{\text{contact}} f_{\theta\theta}^I(0) = 0.758 K_I^{\text{contact}}$, $K_{II}^0 = K_{II}^{\text{contact}} f_{\theta\theta}^{II}(0) = -1.046 K_{II}^{\text{contact}}$. In addition, $g_{r\theta}^I$ and $g_{r\theta}^{II}$ are calculated as $g_{r\theta}^I = f_{r\theta}^I(0)/f_{\theta\theta}^I(0) = 0.535$, $g_{r\theta}^{II} = f_{r\theta}^{II}(0)/f_{\theta\theta}^{II}(0) = -0.152$.

To solve the equations (13a) and (13b) which are the Cauchy singular equations of the first kind, a numerical technique developed by Erdogan et al. (1973) was used. The essential idea of it is to replace the dislocation density function, $B_k(\xi),(k=x,y)$ with a product of the bounded function, $\phi_k(u),(k=x,y)$ and weight function, $w(u)=\sqrt{(1+u)/(1-u)}$. $w(u)$ describes a crack tip singularity where $u=2\xi/c-1$, the normalized ξ with respect to the crack length, c, i.e. $0\leq\xi\leq c\rightarrow-1\leq u\leq+1$. The resultant simultaneous equations from the singular integral equations (13a) and (13b) become

$$\left\{\left[\hat{c}/_2\,(v_k+1)\right]^{\lambda_I-1}+\left[\hat{c}/_2\,(v_k+1)\right]^{\lambda_{II}-1}\right\}+\sigma_{yy}^T(v_k,0)+\sum_{i=1}^n\frac{2\pi(1+u_i)}{2n+1}\left[\phi_x(u_i)\left\{G_{xyy}^{(1)}(v_k,0;u_i,0)+F_{xyy}(v_k,u_i)\right\}+\phi_y(u_i)\left\{G_{yyy}^{(1)}(v_k,0;u_i,0)+F_{yyy}(v_k,u_i)\right\}\right]=0 \tag{14a}$$

$$\left\{g_{r\theta}^I\left[\hat{c}/_2\,(v_k+1)\right]^{\lambda_I-1}+g_{r\theta}^{II}\left[\hat{c}/_2\,(v_k+1)\right]^{\lambda_{II}-1}\right\}+\sum_{i=1}^n\frac{2\pi(1+u_i)}{2n+1}\left[\phi_x(u_i)\left\{G_{xxy}^{(1)}(v_k,0;u_i,0)+F_{xxy}(v_k,u_i)\right\}+\phi_y(u_i)\left\{G_{yxy}^{(1)}(v_k,0;u_i,0)+F_{yxy}(v_k,u_i)\right\}\right]=0, \tag{14b}$$

where $\hat{c}^{\lambda_M-1}=c^{\lambda_M-1}K_M^0\{\pi(\kappa_1+1)/(2G_1)\},(M=I,II)$, and $u_i=\cos[\pi(2i-1)/(2n+1)],(i=1,\ldots,n)$, $v_k=\cos[2k\pi/(2n+1)],(k=1,\ldots,n)$.

The solutions of equations (14a) and (14b) are $\phi_x(u_i)$ and $\phi_y(u_i)$, $(i=1,\ldots,n)$. Then, the crack tip stress intensity factors can be evaluated using the following formulae.

$$K_I^{\text{crack}}=2\sqrt{2}\sqrt{\pi c}\frac{G_1}{(\kappa_1+1)}\phi_y(1),\ K_{II}^{\text{crack}}=2\sqrt{2}\sqrt{\pi c}\frac{G_1}{(\kappa_1+1)}\phi_x(1) \tag{15a,b}$$

where, due to Krenk (1975), $\phi_k(1),(k=x,y)$ is obtained using

$$\phi_k(1),(k=x,y)=\frac{2}{2n+1}\sum_{i=1}^n\left[cot\left\{\left(\frac{2i-1}{2n+1}\right)\frac{\pi}{2}\right\}sin\left\{\left(\frac{2i-1}{2n+1}\right)n\pi\right\}\phi_k(u_i)\right],(k=x,y). \tag{16}$$

EXAMPLE

The cladding crack length, c = 0.1 mm was used for an example calculation. The cladding thermal stress was set as $\sigma_{yy}^T(x,0)$ = 100 MPa tentatively, which was assumed constant along the thickness of the cladding tube. The other values were the same as those used in the contact mechanical analysis. As a result, the mode I and mode II stress intensity factors of the crack, K_I^{crack} and K_{II}^{crack}, respectively, were as follows.

$$\begin{pmatrix}K_I^{\text{crack}}\\K_{II}^{\text{crack}}\end{pmatrix}=\begin{bmatrix}A&B\\C&D\end{bmatrix}\begin{pmatrix}K_I^0c^{\lambda_I-1}\\K_{II}^0c^{\lambda_{II}-1}\end{pmatrix}\sqrt{\pi c}=\begin{bmatrix}A&B\\C&D\end{bmatrix}\begin{pmatrix}f_{\theta\theta}^I(0)\Lambda_I\sigma_o(c/a)^{\lambda_I-1}\\f_{\theta\theta}^{II}(0)\Lambda_{II}\sigma_o(c/a)^{\lambda_{II}-1}\end{pmatrix}\sqrt{\pi c}$$
$$=\begin{pmatrix}12.205\\24.291\end{pmatrix}\ \left(\text{MPa}\sqrt{\text{mm}}\right). \tag{17}$$

where A = 28.7259, B = 28.7134, C = -2.8952 and D = -3.0582. Also, λ_I = 0.508, λ_{II} = 0.807, Λ_I = -1.257, Λ_{II} = 0.4076, σ_o = -10 MPa, a = 3.823 mm as were already evaluated.

CONCLUSION

A novel method of analysing a crack of a fuel rod cladding tube subject to PCMI was developed. It stringently considered a contact of the sharp edge of a cracked pellet fragment with the inner surface of the cladding tube. The orders of stress singularity at the sharp contact edge were found as 0.492 and 0.193 presently. Those will be altered depending on the material, contact angle and contact condition. Stress component equations in the vicinity of the sharp edge were derived from an eigenvalue problem formulation. Pseudo-edge dislocations were imposed on the free boundaries formed in the contact domain as well as for the cladding crack to solve the traction free conditions and the stresses on the crack, respectively. Finally, a numerical technique for solving a singular integral equation was used to obtain the stress intensity factors of the cladding crack. An example calculation showed K_I^{crack} = 12.205 MPa·mm$^{1/2}$ and K_{II}^{crack} = 24.291 MPa·mm$^{1/2}$ if the cladding crack was normal to the cladding inner surface whose length was 0.1 mm, and the thermal stress was 100 MPa.

REFERENCES

Bueckner, H. F. (1958). "The propagation of cracks and the energy of elastic deformation," *Journal of Applied Mechanics*, USA, 80 1225-1230.

Churchman, C. M., Hills, D. A. (2006). "General results for complete contacts subject to oscillatory shear," *Journal of the Mechanics and Physics of Solids*, UK, 54 1186-1205.

Dundurs, J. (1969). "Elastic Interaction of Dislocations with Inhomogeneities," Mathematical Theories of Dislocations, Ed. T. Mura, ASME Publications, USA.

Dundurs, J. Sendeckyj, G. P. (1965). "Behavior of an edge dislocation near a bimetallic interface," *Journal of Applied Physics*, USA, 36 3353-3354.

Erdogan, F., Gupta, G.D., Cook, T.S. (1973). "Numerical Solution of Singular Integral Equations," in *Methods of Analysis and Solutions of Crack Problems*, Ed. Sih, G.C., Noordhoff, Leyden.

Flicek, R. C., Hills, D. A., Dini, D. (2015). "Sharp edged contacts subject to fretting: A description of corner behaviour," *International Journal of Fatigue*, UK, 71 26-34.

Gittus, J. H. (1972). "Theoretical analysis of the strains produced in nuclear fuel cladding tubes by the expansion of cracked cylindrical fuel pellets," *Nuclear Engineering and Design*, UK, 18 69-82.

Hills, D. A., Kelly, P. A., Dai, D. N. and Korsunsky, A. M. (1996). *Solution of Crack Problems,* Kluwer Academic Publishers.

Karuppanan, S., Churchman, C. M., Hills, D. A., Giner, E. (2008). "Sliding frictional contact between a square block and an elastically similar half-plane," *European Journal of Mechanics A/Solids*, UK, 27 443-459.

Kim, H.–K., Hills, D. A., Paynter, R. J. H. (2014). "Asymptotic analysis of an adhered complete contact between elastically dissimilar materials," *Journal of Strain Analysis*, UK, 49 607-617.

Kim, H.–K., Kim, J.–Y. (2014). "Analysis of edge slipping in a complete and adhesive contact of elastically dissimilar bodies subject to normal indentation," *Journal of Mechanical Science & Technology*, Switzerland, 28 2273-2280.

Krenk, S. (1975). "On the use of the interpolation polynomial for solutions of singular integral equations," *Quarterly Applied Mathematics*, USA, 32 479-484.

Marchal, N., Campos, C., Garnier, C. (2009). "Finite element simulation of Pellet-Cladding Interaction (PCI) in nuclear fuel rods," *Computational Materials Science*, UK, 45 821-826.

MATPRO (2001). SCDAP/RELAP5/MOD3.3 Code Manual, NUREG/CR-6150, Vol. 4, Rev. 2, USA.

Nakatsuka, M. (1981). "Theoretical and experimental analyses of cladding strain produced by expansion of cracked fuel pellets," *Nuclear Engineering and Design*, UK, 65 197-204.

Ranjan, G. V. and Smith, E. (1980). "Determination of stress within zircaloy cladding due to pellet-cladding interaction," *Nuclear Engineering and Design*, UK, 56 263-272.

Roberts, G. (1978). "The concentration of stress in cladding produced by the expansion of cracked fuel pellets," *Nuclear Engineering and Design*, UK, 47 257-266.

Sercombe, J., Aubrun, I., Nonon, C. (2012). "Power ramped cladding stresses and strains in 3D simulations with burnup-dependent pellet-clad interaction," *Nuclear Engineering and Design*, UK, 242 164-181.

Walker, S. P., Yu, A., Fenner, R. T. (1992). "Pellet-clad mechanical interaction: pellet-clad bond failure and strain relief," *Nuclear Engineering and Design*, UK, 138 403-408.

Williams, M. (1952). "Stress singularities resulting from various boundary conditions in angular corners of plates in extension," *Journal of Applied Mechanics*, USA, 19 526-528.